Suitability of CASI and ATM airborne remote sensing data for archaeological subsurface structure detection under different land cover: the Arpi case study (Italy)

2010 J. Geophys. Eng. 7 183

(http://iopscience.iop.org/1742-2140/7/2/S04)

J. Geophys. Eng. **7** (2010) 183–189 doi:10.1088/1742-2132/7/2/S04

Suitability of CASI and ATM airborne remote sensing data for archaeological subsurface structure detection under different land cover: the Arpi case study (Italy)

S Pascucci, R M Cavalli, A Palombo and S Pignatti

National Research Council, Institute for Atmospheric Pollution (CNR IIA-LARA) and Institute of Methodologies for Environmental Analysis (CNR IMAA), Via Fosso del Cavaliere 100, 00133, Roma, Italy

E-mail: pascucci@imaa.cnr.it

Received 31 July 2009
Accepted for publication 9 November 2009
Published 4 May 2010
Online at stacks.iop.org/JGE/7/183

Abstract

In this paper multi-sensor airborne remote sensing has been applied to the Arpi archaeological area of southern Italy to assess its suitability for detecting and locating subsurface archaeological structures and to delineate subsurface remains beyond the current limits of ground geophysical data. To this aim, the capability of CASI and ATM reflectances in the VIS–NIR spectral range and the ATM apparent thermal inertia for subsurface archaeological prospection have been assessed at different sites of the Arpi archaeological area. First, linear spectral mixture analysis has been applied to CASI and ATM images to retrieve the dominant land cover for the selected subsurface structures, and then, the spectral bands most effective for the archaeological buried structure detection as a function of the land cover characteristics have been evaluated. The results reveal that multi/hyperspectral airborne remote sensing data can represent an effective and rapid tool to detect subsurface structures within different land cover contexts. Therefore, the proposed methodology can be used to perform a preliminary analysis of those areas where large cultural heritage assets occur by prioritizing and localizing the sites where to apply archaeological prospection.

Keywords: hyperspectral imagery, airborne remote sensing, subsurface archaeological structures, anomalies, photo-interpretation

1. Introduction

The massive developments and changes to the landscape induced by human growth make it necessary to develop efficient and cost-effective methods to find, map and attain information from sites of our cultural heritage (Kvamme 2005). Viewing archaeological structures and/or subsurface remains from ground level generally does not clearly identify the spatial characteristics of these structures or the relationship with surrounding archaeological sites. To this aim, the application of remote sensing data for detecting subsurface structures is becoming a remarkable tool for the archaeological observations to be combined with the near surface geophysics (Kvamme 2005, Kucukkaya 2004). Different satellite and airborne sensors have been used for archaeological applications, such as the identification of spectral anomalies (i.e. marks) related to the buried remnants within archaeological sites, and the management and protection of archaeological sites (Buck *et al* 2003, Lasaponara and Masini 2007, Rowlands and Sarris

2007, Gallo *et al* 2009). In particular, airborne remote sensing allows us to rapidly investigate archaeological areas; it can detect features relative to subsurface remains unseen before, precisely map them and offer interpretations based on their form, distribution and context (Kucukkaya 2004, Buck *et al* 2003, Rowlands and Sarris 2007). Although presenting opportunities to the archaeological community, these sensors have their disadvantages that also need to be taken into account (Rowlands and Sarris 2007). First, it is to be remarked that the remote sensing detectability of permanent surface spectral features (labelled as 'marks') due to buried structures, i.e. to the alteration of the natural trend of superficial soil and/or vegetation growth, is affected by the following factors: (1) the spectral contrast between the target and background materials, (2) the dimension and fraction of the target in relation to the background, (3) the imaging system characteristics being used (bands, instrument noise and pixel size), (4) the land cover type and condition under which these structures lie (i.e. the compaction of soil, moisture content and vegetation type and structure) and (5) the conditions under which the surface is being imaged (i.e. illumination and atmospheric conditions) (Lasaponara and Masini 2007). The combination of these factors defines the pixel appearing with differences, with respect to the adjacent pixels, in colour, texture, brightness and spectral feature behaviour (Cavalli *et al* 2007). Second, most applications utilizing remote sensing within archaeology take a single sensor approach, whereas the real benefits with respect to the archaeological interpretation will be achieved through a multi-sensor approach exploiting the different qualities of each sensor (Rowlands and Sarris 2007).

In this framework, the paper stresses the importance of the spectral information to evaluate different airborne imagery capability in terms of detection potential of archaeological spectral anomalies related to subsurface remnants covered by different land cover. To this aim, the spectral information of Compact Airborne Spectrographic Imager (CASI) and Airborne Thematic Mapper (ATM) multi/hyperspectral airborne sensors with respect to the dominant land cover surfacing known and unexcavated archaeological subsurface structures (e.g. stone walls and pavements near the surface) has been analysed and compared to assess their effectiveness in subsurface structure detection.

Starting from certain training information attained by Cavalli *et al* (2005, 2009) for multispectral infrared visible imaging spectrometer (MIVIS) data in the Arpi archaeological area, 25 pairs of regions of interest (ROI) encompassing the spectral anomaly–background system (marks) (Cavalli *et al* 2005) related to subsurface remains were manually delineated on CASI and ATM images. Spectral mixture analysis was used to assess CASI and ATM images, the land cover fractional abundances surfacing the chosen buried remains. Next, a spectral separability index was applied to determine the CASI and ATM suitable spectral bands to detect subsurface remains in relation to the surfacing land cover.

Comparison results for the CASI and ATM sensors bear out that the proposed methodology applied to airborne multi/hyperspectral remote sensing data can represent an effective and rapid tool to detect subsurface remains.

2. Study area and data

To demonstrate the effectiveness of the two proposed airborne multi/hyperspectral sensors, a well-established (Cavalli *et al* 2005, 2009, Bradford 1957) test site of the Arpi archaeological area (southern Italy) is presented.

The Arpi archaeological area encompasses an ancient city of Apulia located 8 km NE of the modern city of Foggia in a prevailing agricultural area. This area is considered the metropolis of the ancient Daunia (Greek place name, 'Argyripta') (Bradford 1957). Strabo says that from the extent of the city walls one could gather that it had once been one of the greatest cities of Italy. As a protection against the Samnites, Arpi became an ally of Rome (320 BC) and remained faithful until after the battle of Cannae. Arpi was then ruined by the Saracens in the 11th century, and according to medieval sources, it was populace of Arpi who settled nearby Foggia. Excavations begun in the 1940s discovered the foundations of Hellenic–Roman buildings showing pretty mosaic floors. A necropolis was also found, with many graves and small cave burials, with examples of Apulian vases with their red figures and geometric decorations, dating from between the fourth and third century BC. The most important remnants are the ancient city stone walls.

For this area, previous studies performed by Cavalli *et al* (2005, 2009) had identified on MIVIS imagery spectral anomalies related to subsurface archaeological structures and the optimal MIVIS wavelength bands to detect the following not yet excavated archaeological structures: an ensemble of features relative to the whole ancient city external perimeter wall (the 'aggere', about 10 km), two features relative to the defensive structures along the perimeter (i.e. stone walls) and some features relative to the main stone streets entering into the ancient metropolis.

The site was, therefore, chosen for the current study since it contains known subsurface archaeological remains, has existing detailed geophysical and archaeological data locating buried archaeological features within 1 and 3 m of the surface and has relatively low vegetation densities with areas of exposed soil in a main agricultural area, which is covered by MIVIS, CASI and ATM airborne multi/hyperspectral images.

The CASI and ATM (figure 1) airborne imagery was acquired over a 2 day period with eight CASI and six ATM stripes acquired on 25 April 2005 at 13:50, and three ATM night stripes acquired in order to gauge diurnal heat capacity on 26 April 2005 at 03:06, as part of the Natural Environment Research Council (NERC, UK) Mediterranean Flight Campaign. The study area corresponds to a CASI and ATM resized image of 1700 × 5000 pixels (i.e. about 3400 × 10 000 m) as depicted in figure 1.

The CASI sensor is limited to the visible and near infrared (NIR) and was programmed to operate in spatial mode acquiring data in 48 channels from 449 nm to 940 nm at a spatial resolution of 2.0 m, whilst the ATM sensor acquired data in 11 broader bands, with a spatial resolution of 2.0 m. The ATM sensor provides important information in the short wave infrared (SWIR) and the thermal (TIR) portions of the

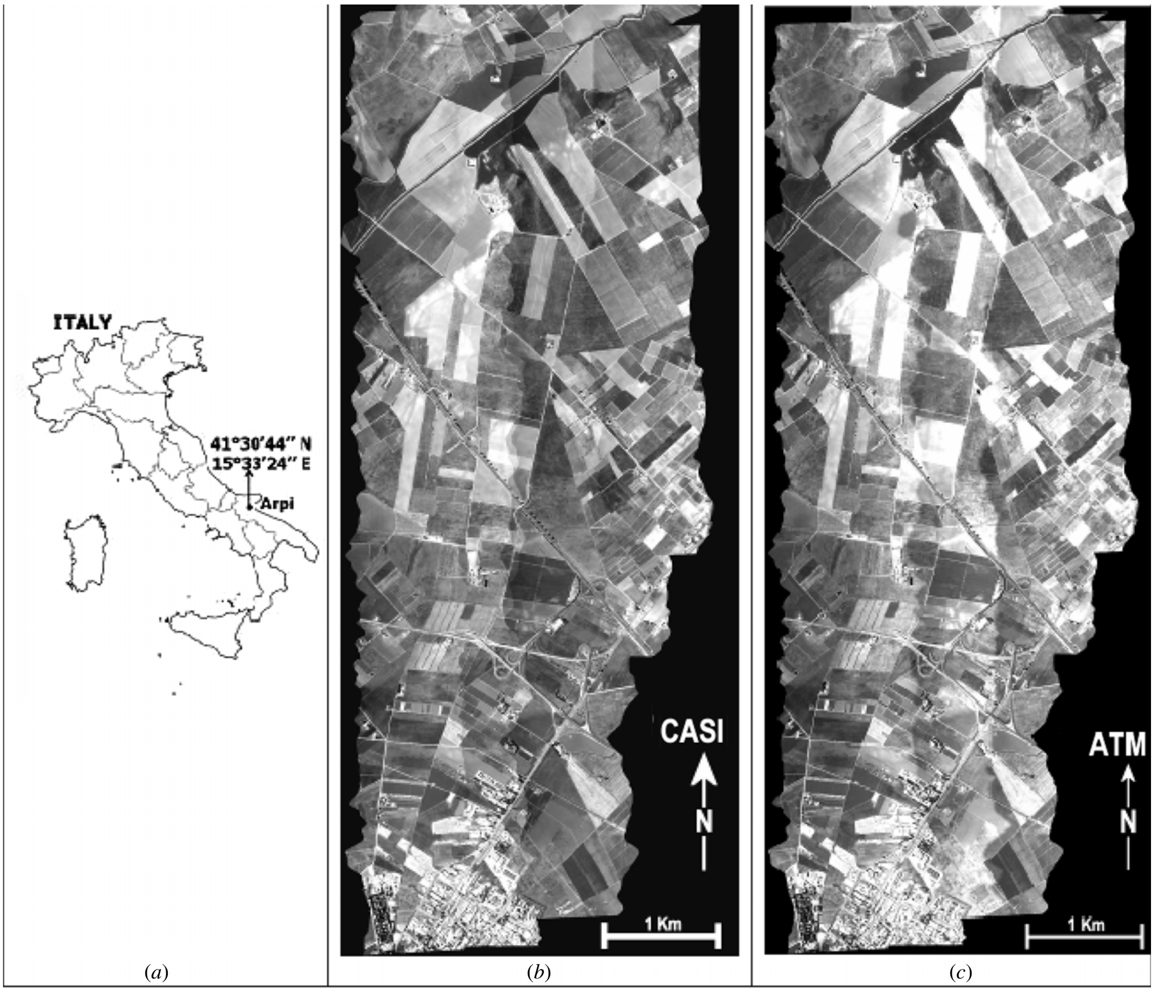

Figure 1. (*a*) Location of the Arpi study area over a regional map. (*b*) CASI and (*c*) ATM stripes acquired on the Arpi archaeological area (CASI and ATM mosaic of the images at 0.66 μm are depicted only for visualization purposes).

Table 1. Characteristics of CASI and ATM sensors used for this study.

	Spectral region	Spectral resolution (μm)	Spectral range (μm)	Spatial resolution (m)	IFOV (deg)	Swath width
CASI	VNIR (48 ch.)	0.019	0.40–0.80 (VIS) 0.81–0.95 (NIR)	≅2	1.0 mrad	512 spectral pixels
ATM	VNIR (9 ch.)	0.02 (VIS) 0.05 (NIR)	0.42–0.90 0.91–1.75	≅2	2.5	Pixel swath 938
	SWIR (1 ch.)	–	2.08–2.35			
	TIR (1 ch.)	–	8.5–13.0			

spectrum with respect to soil properties and heat capacity (Rowlands and Sarris 2007). The main characteristics of the CASI and ATM sensors are summarized in table 1.

3. Methods

3.1. Test sites selection

The test sites were chosen in the Arpi archaeological area since they (a) include subsurface archaeological remains unexcavated, with a sharp geometry and covered by CASI and ATM airborne multi/hyperspectral remote sensing data acquired with similar atmospheric conditions, at low solar zenith angle and with similar soil moisture dryness conditions, and (b) have existing detailed geophysical and archaeological data locating buried archaeological features (Cavalli *et al* 2005, 2009).

For each of the 25 selected test sites, two ROIs, one relative to the known marks identified by archaeologists (Cavalli *et al* 2005, 2009) and one to the marks' surrounding background, were manually delineated on CASI and ATM airborne imagery to be further analysed by using the SI index.

These ROIs point up only homogenous land cover both for the mark and background and are characterized by a spatial extent of at least 60 m^2 for the mark and no less than 120 m^2 for the background.

3.2. Airborne data pre-processing

For this study, CASI and ATM airborne remote sensing data were processed.

First, CASI and ATM radiances were corrected to reflectance using the FLAASH module incorporating the MODTRAN4 radiation transfer code (Matthew *et al* 2000) in the ENVI software package.

Second, CASI and ATM airborne data were geometrically corrected by using an own code based on the precise trajectory reconstruction process by using onboard GPS/INS systems of the two airborne and additional ground control point information to compensate for aircraft position, altitude and ground surface separation. A mean RMS error of 1 pixel was attained for each image of CASI and ATM datasets so enabling their mosaicking and precise comparison for the further processing results between the classified imagery, which can be influenced by the accuracy of the pixels' location (RMS error).

Finally, on the ATM TIR data, the apparent thermal inertia (ATI) as proposed by Price (1985) was calculated. However, the ATI is only applicable to those sites covered by bare soil or regions with low crop vegetation. In general, the thermal inertia is given by the formula $P = \sqrt{Kc\rho}$, where K is the thermal conductivity, c is the specific heat and ρ is the density of the material, and it describes the resistance of a material to the change in its temperature. The thermal inertia is approximated by the ATI that can be obtained by using remote sensing thermal images (Price 1985). The ATI is defined as

$$\mathrm{ATI} = NC_1(1-\alpha)/(\Delta T) \tag{1}$$

where N is the scaling factor, α is the apparent albedo, as obtained by CASI daytime atmospherically corrected images, ΔT is the temperature difference calculated on ATM thermal images acquired during the night and the day passes and C_1 is defined as

$$C_1 = \sin\vartheta \sin\varphi(1-\tan^2\vartheta \tan^2\varphi) + \cos\vartheta \cos\varphi ar\cos(-\tan\vartheta \tan\varphi) \tag{2}$$

where ϑ is the latitude and φ is the solar declination.

3.3. Imagery classification

To verify the potentialities of the airborne multi/hyperspectral sensors in detecting archaeological spectral anomalies (marks) related to subsurface remains covered by two different land covers, which was performed by evaluating the spectral contrast between the known marks and the surrounding background, the following processing methodology was applied to the whole multi-sensor dataset: (1) spectral unmixing (LSU), (2) spectral separability index (SI) calculation on a CASI and ATM per band basis and (3) plot analysis of the SI versus land cover fractional abundances (i.e. LSU results).

First, a constrained spectral mixture analysis (Small 2001, Settle and Drake 1993, Chan 2003) trained with the dry bare soil and green crop endmembers was used within the ENVI software package. The endmembers used depend on the nature of the scene, as well as the spatial scale, spectral resolution and number of spectral bands in the image (Small 2001, Settle and Drake 1993). These two endmembers were defined by Cavalli *et al* (2009) for the same test sites in their study and chosen for this research, as they depict the land cover variability on the 25 test sites. Mathematically, linear mixing comprises linear combinations of component (endmember) spectra:

$$r = Mf_N + \varepsilon \tag{3}$$

where r is the column vector of the measured radiance/reflectance spectrum with L spectral bands, M is the $L \times N$ endmember spectra matrix (N is the number of pure endmembers), f_N is the concentration vector whose components represent the endmember fraction for each endmember and ε is the residual error. In this model, M is known, while the unknown to be retrieved is the concentration f_N.

Alternatively, it is to be considered that different techniques for automatic endmember extraction from hyperspectral data can be applied to the same purpose. When no references (e.g. spectra from *in situ* measurements or from spectral libraries) are available, the analyst must derive the endmembers directly from the data cube (see e.g. the Pixel Purity Index, the Orasis, the N-FINDR and the Iterative Error Analysis algorithms), which is not an obvious task (Chan 2003). In fact, the major drawback of all these approaches is that they only take into account the spectral information contained in the data cube, disregarding spatial information.

Second, the separability spectral index (SI) described by Cavalli *et al* (2007), and here briefly recalled, was used to rank the capability of detecting the archaeological spectral anomalies by a per-band basis on the airborne data. The SI index describes, for the 25 test sites (i.e. the 25 pairs of ROI encompassing the spectral anomaly–background systems), the total differences between the frequency distributions of spectral anomaly pixels and the pixels selected as the background for the same spectral anomalies, and it is defined as a normalized scalar product expressed as follows:

$$SI = \left(1 - \frac{\int D_{\mathrm{marks}} D_{\mathrm{background}}\,\mathrm{d}x}{\sqrt{\int D^2_{\mathrm{marks}}\,\mathrm{d}x \int D^2_{\mathrm{background}}\,\mathrm{d}x}}\right) \times 100 \tag{4}$$

where D_{marks} represents the frequency distribution of the digital values of those pixels belonging to the archaeological spectral anomalies (marks) in all images, while $D_{\mathrm{background}}$ corresponds to the frequency distribution of those pixels selected as the background.

Finally, plot analysis (Chan 2003) of the SI values calculated for each CASI and ATM band with respect to the LSU results (i.e. to the fractional abundances of the two endmembers of the mark–background systems) was used to show up which are the spectral bands maximizing the archaeological signatures and to verify the correctness of the procedure proposed by Cavalli *et al* (2007, 2009) for the same archaeological area using MIVIS airborne imagery.

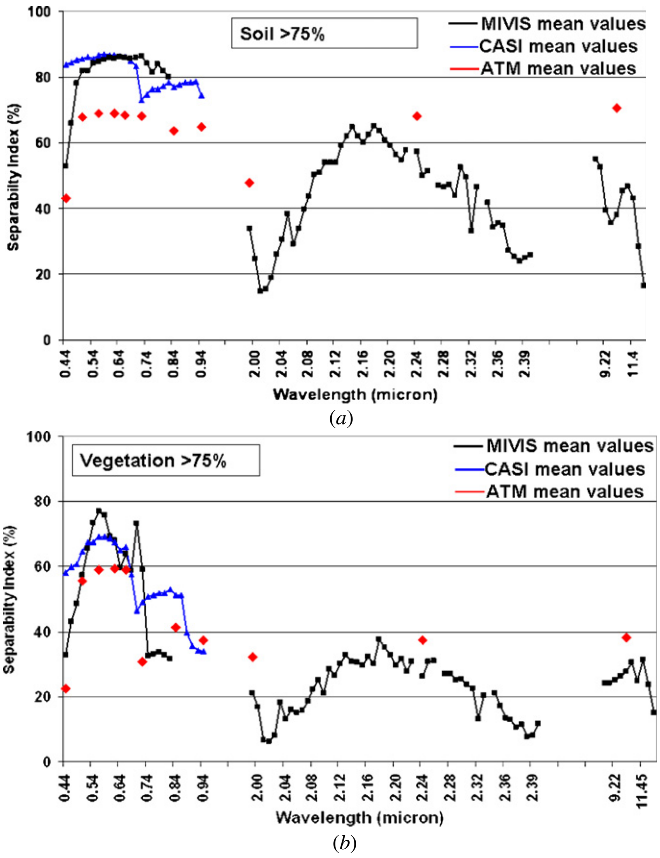

Figure 2. Plot analysis of the unmixing versus SI results for CASI and ATM sensors compared with MIVIS ones attained for two different land cover conditions: (*a*) archaeological subsurface structures covered by more than 75% of dry bare soil, and (*b*) covered by more than 75% of green crop vegetation (the ATM thermal results are reported in red in both graphs as ATI mean values only for visualization purposes).

4. Results and discussion

Bare soil and photosynthetic green crops were applied as endmembers in the LSU procedure of CASI and ATM imagery by constraining the fractions to sum to 1. The 'shade endmember' was not included in each endmember model to account for variation in illumination, as the 25 marks were not significantly affected by shadowing (i.e. the data were recorded in sun with maximum elevation).

The unmixing results for the CASI and ATM remote sensing data on the selected Arpi test sites (i.e. 25 ROIs with 3120 pixels known to be marks and 11 245 pixels selected as the background used for computing the SI) are in accordance with those attained by Cavalli *et al* (2009) for MIVIS data (see figure 2), thus confirming that the spectral mixture analysis can be applicable to describe the wide range of anomaly–background systems used for this study also for images acquired by different airborne sensors (i.e. MIVIS, CASI and ATM).

Plot analysis of SI values versus the fractional abundances of the two endmembers was used to highlight the optimal CASI and ATM bands exploiting the archaeological signatures for multi/hyperspectral airborne remote sensing imagery (figure 2) within different land covers with different fractional abundances.

Plot analysis of the unmixing versus SI results for the two sensors allowed us to establish that for the land cover characterized by green crop vegetation that was set as the occurrence of green crop vegetation higher than 75%, the VIS–NIR spectral regions better enhance the buried man-made structures thus confirming the results attained by Cavalli *et al* (2009) in previous studies. In particular, the two most promising wavelengths for their detection are the chlorophyll peak at 0.56 μm and the red edge region (0.66 to 0.70 μm) (see e.g. in figures 3(*a*)–(*c*), the test sites 2 and 3). This result also confirms that the variation induced by the subsurface structures (e.g. stone walls, road networks) to the natural vegetation growth and/or colour (i.e. for different stress factors) is primarily detectable by the chlorophyll peak and the red edge region. Actually, the transition between two regions at approximately 0.7 μm is characterized by the red edge of the chlorophyll absorption maximum, and the leaf reflectance is controlled in the visible to 0.7 μm by the pigments in the leaves. In the region 0.7 to 1.3 μm, the dominant feature is the high, relative reflectance associated with leaf cell structure and is associated with the cellular arrangement within the leaf and the hydration state. The exact position of the red edge is changed in plants influenced by geochemical stress.

As regards the test sites where dry bare soils cover the structures with fractions higher than 75% from the unmixing results, all the VIS, NIR and SWIR spectral regions are suitable to detect the subsurface structures (see e.g. in figures 3(*a*)–(*d*) the test site 1).

The ATM TIR (see e.g. in figure 3(*e*)) spectral region (8.5–13.0 μm) provided useful results in terms of subsurface structure detection only for the calculated ATI (thermal inertia) whenever the structures are covered by dry bare soil for more than 75%, instead ATM TIR data provided only SI values under 40% for the structures covered by soils more than 75% and under 25% for the structures covered by crop vegetation more than 75%. However, we believe that the ATM TIR spectral properties of subsurface archaeological structures have not been fully exploited in this study as ATM TIR data, even if with only one channel, allows for an effective detection of archaeological subsurface structures covered by soil or crop vegetation. This is because the heat transfer through the soil is affected by the presence of buried objects; thus, it is of primary importance to calculate the material inertial resistance to temperature fluctuations for detecting the subsurface remains.

Last, we verified on other known (Cavalli *et al* 2005, 2009, Bradford 1957) buried structures within the Arpi archaeological area that if over the subsurface structures crop up a mixture of bare soil and green crop, as identified by the LSU results, there will be a loss in terms of subsurface structure detection potential of all CASI and ATM bands.

In conclusion, looking at the graphs in figure 2 it is possible to state that a multi/hyperspectral airborne sensor covering the 0.55–0.75 μm spectral range (VIS–NIR) with high spectral (0.1–0.3 μm) and spatial (i.e. at least

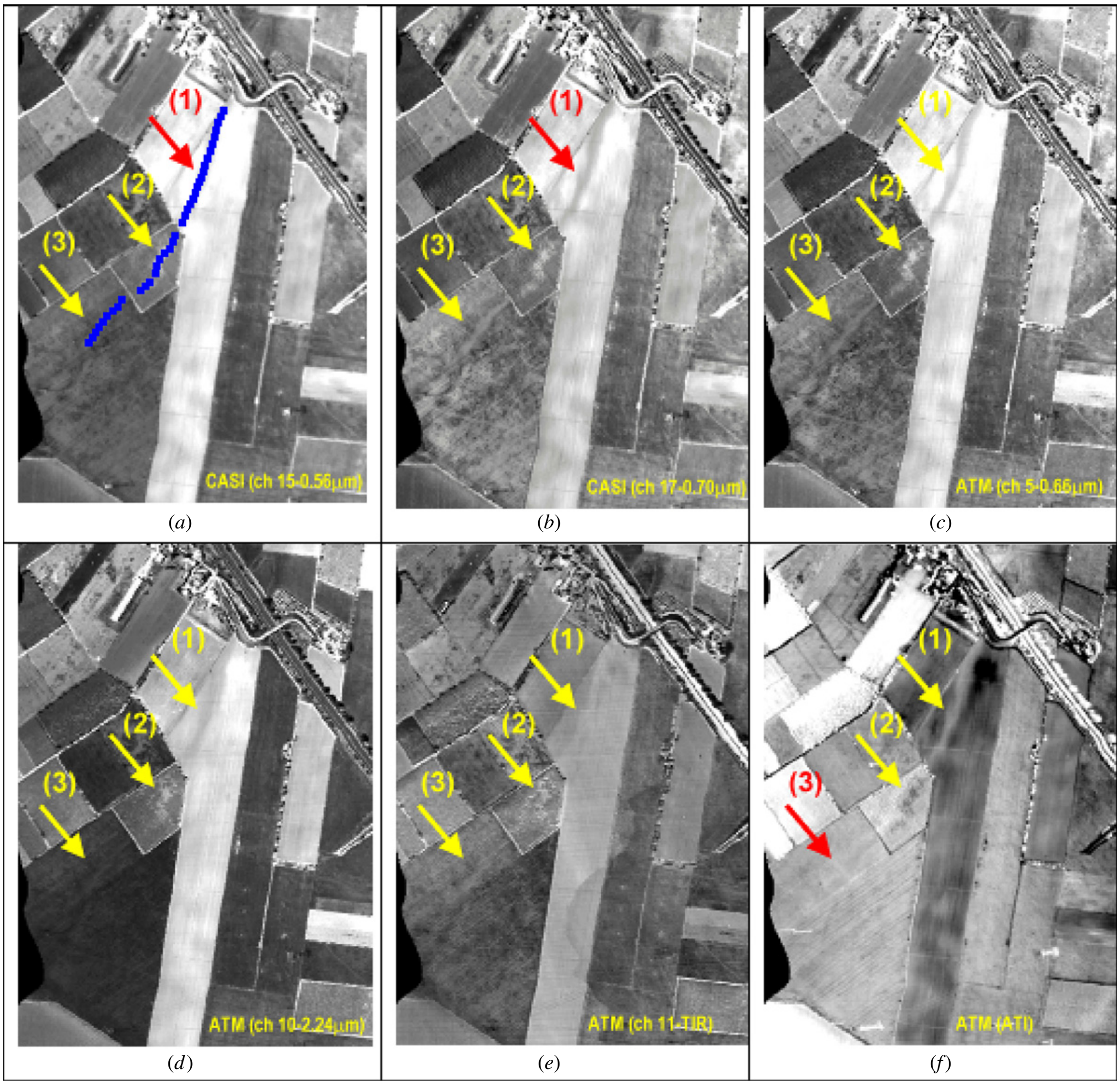

Figure 3. Examples of CASI and ATM bands selection as derived by applying the proposed procedure and suitable for detecting subsurface structures on three selected test sites within the Arpi archaeological area. For the three test sites the pixels known to be marks used for computing the SI are 124 and they are depicted in blue in (*a*) only for visualization purposes.

2–3 m/pixel) resolutions can be suitable for subsurface archaeological structure detection each time the surfacing fractional land cover is well known, thus confirming previous results attained for the same area by MIVIS hyperspectral airborne data (see figure 2).

Looking at the ATM thermal data classification, they provide appreciable results in discriminating subsurface structures covered by soil more than 75% (see ATM ATI values in figure 2(*a*)). This is also confirmed by comparing the results with previous results obtained by MIVIS TIR data for the same test areas and with the same atmospheric conditions (Cavalli *et al* 2009). Probably the better results obtained by the ATM TIR data are due to (a) the higher spatial resolution of the ATM data (2 m/pixel) with respect to the MIVIS one (3 m/pixel), (b) different time and season of acquisition and (c) soil moisture and roughness. Furthermore, the calculation on ATM TIR night and day dataset of the thermal inertia (see e.g. figure 3(*f*)) provided, as expected, appreciable results only in those sites (i.e. marks relative to subsurface remains) covered by more than 75% by dry bare soil, thus sustaining that the ATI calculation is useful where dry bare soil covers the subsurface structures. Moreover, it is to consider that we used the simplified equation of apparent thermal inertia, where only surface albedo and surface day–night temperature difference are considered, and surface latent flux, surface sensible flux and other atmosphere parameters are neglected thus leading to higher error occurrences. However, the ATI SI mean values attained for all the test sites are higher than those for the ATM TIR night and day data.

5. Conclusions

In this paper we test and demonstrate with different spectral resolution airborne imagery that the combined use of the separability index and the land cover fractional abundance (as derived by spectral unmixing) is a powerful technique to identify the sensors' bands most profitable for archaeological prospection. The results attained for the selected Arpi (Italy) test area reveal that if the dominant land cover abundances in agricultural land areas are known, we can *a priori* select the optimal spectral range for remote sensing data suitable for the enhancement of spectral anomalies related to the subsurface archaeological remains. Furthermore, the results show that high spatial resolution VNIR multi/hyperspectral data, such as CASI and ATM airborne data, can be extremely effective for the analysis of large cultural heritage assets. The usefulness of the ATI (thermal inertia) where archaeological structures are covered by bare soil is also noteworthy.

At present, the only possibility of improving the attained results is the application of hyperspectral imagery with a very high spatial resolution (if possible <1 m) also in conjunction with LIDAR and/or high resolution SAR data such as the new COSMO-SkyMed SAR data. In this context, the COSMO-SkyMed data are expected to represent a precious source of information thanks to the high spatial resolution of the images (at maximum 1 m) acquired, to the very short revisit time and to the low sensitivity, typical of synthetic aperture radar (SAR) data, to atmospheric and sun-illumination conditions.

Further research will include the evaluation of the effectiveness and robustness of the proposed procedure in the same and other archaeological areas by including more endmembers in the unmixing procedure.

This will allow us to develop a quick and affordable tool for archaeologists whenever starting their analysis on airborne remote sensing data with scarce information and to improve the standard methods employed in landscape research, from creating archaeological risk maps to assembling regional information systems. However, the relatively high costs of high spatial/spectral remote sensing data must be balanced against the real larger costs of planning decisions based on poor knowledge of what lies in the subsurface and of failing to correctly locate archaeological features and other culturally sensitive deposits prior to their disturbance.

References

Bradford S 1957 The ancient city of Arpi in Apulia *Antiquity* **31** 167–9

Buck P E, Sabol D E and Gillespie A R 2003 Sub-pixel artifact detection using remote sensing *J. Archaeol. Sci.* **30** 973–89

Cavalli R M, Colosi F, Palombo A, Pignatti S and Poscolieri M 2007 Remote hyperspectral imagery as a support to archaeological prospection *J. Cult. Herit.* **8** 272–83

Cavalli R M, Merola P, Pignatti S and Poscolieri M 2005 Telerilevamento iperspettrale MIVIS per lo studio delle testimonianze antropiche nell'area archeologica di Arpi (FG) Italia *Riv. Ital. Telerilevamento* **33**/**43** 711–901

Cavalli R M, Pascucci S and Pignatti S 2009 Optimal spectral domain selection for maximizing archaeological signatures: Italy case studies *Sensors* **9** 1754–67

Chan C I 2003 *Hyperspectral Imaging: Techniques for Spectral Detection and Classification* (Dordrecht: Kluwer)

Gallo D, Ciminale M, Becker H and Masini N 2009 Remote sensing techniques for reconstructing a vast Neolithic settlement in Southern Italy *J. Archaeol. Sci.* **36** 43–50

Kucukkaya A G 2004 Photogrammetry and remote sensing in archaeology *J. Quant. Spectrosc. Radiat. Transfer* **97** 83–97

Kvamme K L 2005 *Terrestrial Remote Sensing in Archaeology* ed H Maschner and C Chippindale (Lanham, MD: AltaMira Press) pp 1–23

Lasaponara R and Masini N 2007 Detection of archaeological crop marks by using satellite QuickBird multispectral imagery *J. Archaeol. Sci.* **34** 214–21

Matthew M W *et al* 2000 Status of atmospheric correction using a MODTRAN4-based algorithm *Proc SPIE* **4049** 199–207

Price J C 1985 On the analysis of thermal infrared imagery: the limited utility of apparent thermal inertia *Remote Sens. Environ.* **18** 59–73

Rowlands A and Sarris A 2007 Detection of exposed and subsurface archaeological remains using multi-sensor remote sensing *J. Archaeol. Sci.* **34** 795–803

Settle J J and Drake N A 1993 Linear mixing and estimation of ground cover proportions *Int. J. Rem. Sens* **14** 1159–77

Small C 2001 Estimation of urban vegetation abundance by spectral mixture analysis *Int. J. Rem. Sens.* **22** 1305–34